Editors' Suggestion | Featured in Physics

Experimental Verification of a Bigrating Beam Rider

Ying-Ju Lucy Chu,[1] Nelson V. Tabiryan,[2] and Grover A. Swartzlander, Jr.[1*,†]
[1]Chester F. Carlson Center for Imaging Science, Rochester Institute of Technology, Rochester, New York 14623, USA
[2]BEAM Engineering for Advanced Measurements, Winter Park, Florida 32810, USA

(Received 11 September 2019; published 13 December 2019)

An optical beam rider making use of a light sail comprising two opposing diffraction gratings is experimentally demonstrated for the first time. We verify that the illuminated space-variant grating structure provides an optical restoring force, exhibiting stable oscillations when the bigrating is displaced from equilibrium. We further demonstrate parametric cooling by illuminating the sail with synchronized light pulses. This experiment enhances the technical feasibility of a laser-driven light sail based on diffractive radiation pressure.

DOI: 10.1103/PhysRevLett.123.244302

Light-driven sails navigate through space by transferring momentum from natural light sources such as the Sun or engineered sources such as lasers to the sailcraft. Motivated by the potential to reach solar escape velocities or relativistic speeds, laser-driven sails have attracted considerable scientific attention over the past several decades [1–11]. Modern photonic metamaterial technologies offer the potential to create thin actively controlled diffractive films that provide optomechanical characteristics such as a high momentum transfer efficiency and switching between diffraction orders. A uniform passive diffraction grating provides a force that is independent of the illumination point [12–14]. In contrast a space variant grating such as a "bigrating" [15], and variants thereof [16], may provide a position-dependent force. Thus a space-variant grating may be designed to function as a "beam rider". A laser-driven beam rider must produce self-action both to pull the sail into the beam path when disturbed and to inhibit tumbling [8,17–20].

Here we report on a fundamental experiment that verifies the predicted optomechanical stability provided by a diffractive light sail. We demonstrate that a bigrating comprising two adjacent grating panels having equal and opposite grating vectors provides a position-dependent restoring force. Furthermore we prove that the system may be used as a parametric oscillator, allowing forced damping [21–24], excitation [25,26], or control [27,28] by use of a time-varying laser beam. The latter opens new opportunities for both space and terrestrial applications such as energy harvesting, optomechanical cooling (described below), and photonic sensing [29,30]. The bigrating model in this Letter, which is constrained to 1 degree of freedom, may be generalized to a fully space-variant structure having 3 degrees of freedom, which is beyond the scope of this Letter.

The optomechanics of a bigrating diffractive beam rider may be understood by examining Figs. 1(a) and 1(b), which depict two diffractive panels (A and B), each of width L. Ideally each panel diffracts the incident beam of half-width w_0 into a single diffraction order, as depicted, resulting in positive (negative) components of radiation pressure force F_x on panel A (B). A stable equilibrium point is expected at $x = 0$, i.e., when the beam equally illuminates both panels. Both panels experience the same longitudinal component of force F_z (not shown), which does not affect our experiment and is therefore ignored below [13].

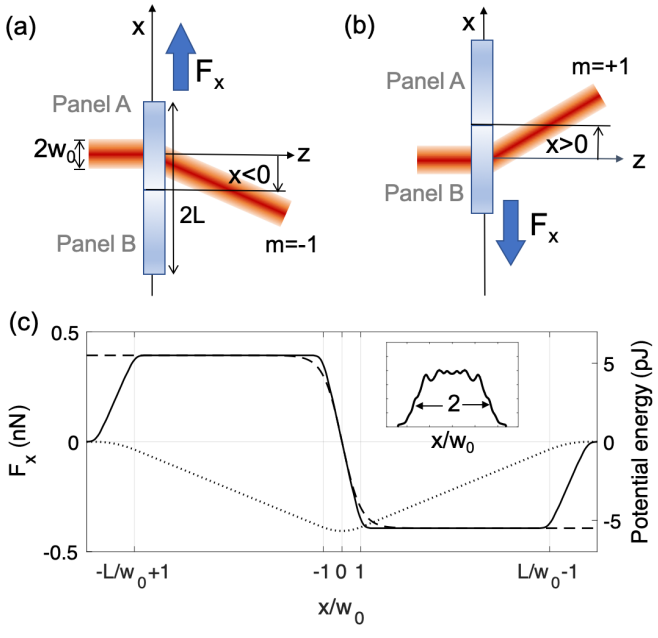

FIG. 1. Transverse restoring force vs displacement of the bigrating. Laser of radial size w_0 illuminating (a) panel A ($x < 0$) and (b) panel B ($x > 0$). (c) Position-dependent force profile calculated from Eq. (1) (solid line) and the "tanh" model (dashed line). Potential energy landscape (dotted line). (Inset) Integrated beam profile of measured beam $\int g(x, y)dy$.

The position-dependent force profile on a given panel is related to the overlap integral of the measured beam intensity profile $I(x,y) = P_i g(x,y)$ across the respective panel, where P_i is the incident beam power, and $g(x,y)$ is the normalized profile function: $\int g(x,y)dxdy = 1$. Assuming that the beamwidth is smaller than the panel size, $w_0 < L$, and that the beam is centered on the panels in the y direction, the net force may be expressed:

$$F_x(x) = F_{x,A} + F_{x,B}, \tag{1a}$$

$$F_{x,A} = F_0 \int_{-L}^{L}\int_{-L}^{0} g(x-x';y)dx'dy, \tag{1b}$$

$$F_{x,B} = -F_0 \int_{-L}^{L}\int_{0}^{L} g(x-x';y)dx'dy, \tag{1c}$$

$$F_0 = \eta\lambda P_i/\Lambda c, \tag{1d}$$

where F_0 is a scaling force [12], c is the speed of light, and $\eta = \sum_m \eta_m m$ is the diffractive force efficiency, where $\eta_m = P_m/P_i$ and where P_m is the power diffracted into the mth order (see Table I). The force near the equilibrium point at $x = 0$ may be approximated

$$\tilde{F}_x(x) \approx -F_0 \tanh(x/w_0), \tag{2}$$

as illustrated by the dashed line in Fig. 1(c). For the measurements described below, $\eta = 0.73$, $\lambda = 808$ nm is the forcing laser wavelength, and $\Lambda = 6$ μm is the grating period. For example, the position-dependent force depicted in Fig. 1(c) (solid line) was determined for a beam of width $w_0 = 2.1$ mm and panels of widths $L = 12.7$ mm. The potential energy associated with this force, plotted in Fig. 1(c) (dotted line), indicates an equilibrium point at $x = 0$, as expected.

Near equilibrium, the bigrating experiences a restoring force with an approximate radiation pressure stiffness

$$K_{\mathrm{RP}} = -dF_x/dx|_{x=0} \approx -d\tilde{F}_x/dx|_{x=0} = F_0/w_0. \tag{3}$$

We find that the approximate stiffness value agrees with the experimentally determined value (described below) to within 4%: $K_{\mathrm{RP}} = (1.9 \pm 0.2) \times 10^{-7}$ N/m for a beam of width $w_0 = 2.1 \pm 0.05$ mm.

TABLE I. Experimentally determined fractional power for mth order diffraction η_m, specular reflection $\eta_{r,0}$, and diffuse scattering η_s.

	η_{-2}	η_{-1}	η_0	η_1	η_2	$\eta_{r,0}$	η_s
Panel A	0.006	0.773	0.015	0.051	0	0.107	0.048
Panel B	0	0.051	0.015	0.773	0.006	0.107	0.048

We designed a micrometer thin space variant bigrating comprising nematic liquid crystals having its anisotropy axis—the director—rotated in the grating plane over a spatial period Λ [Figs. 2(a) and 2(b)]. The cycloidal rotation directions are opposing in panels A and B [Fig. 2(c)], resulting in equal and opposite grating vectors [31] for a circularly polarized beam of light. The diffraction efficiency of such gratings theoretically reaches 100% for radiation wavelength meeting half-wave retardation condition. To provide structural support, the layer was adhered to a 100 μm thick polymer film. The net mass of the square 25.4×25.4 mm^2 bigrating was $M_g = 0.12$ g. Owing to the opposite handedness of the director rotation, a circularly polarized incident beam diffracts in opposite directions, as depicted in Figs. 1(a) and 1(b). For a beam at normal incidence, the dominant first order diffraction angles are given by $\theta_{\pm 1} = \pm\sin^{-1}(\lambda/\Lambda) = \pm 7.74°$. We get 91.5% of the unscattered, transmitted light into the ∓ 1 order for panels A and B.

To observe the reaction of the bigrating to either a constant or a time-varying beam of light, we attached it to one arm of a torsion oscillator at a vacuum pressure of 1.4×10^{-6} Torr $= 1.8 \times 10^{-4}$ Pa, as depicted in Fig. 3 (the other half of the torsion arm which includes a balancing mass is not shown). The torsion arm of length $R = 0.11$ m was suspended by a 25 μm diameter tungsten filament of length 0.24 m. A small mirror was attached to the torsion arm at the pivot to provide a means of measuring the deflection angle 2ϕ of a low power tracking laser beam. Time-lapse photographs of the tracking beam were recorded on a screen at a distance $D = 1.75$ m. A small angular displacement of the bigrating, ϕ, produces a lateral displacement of the tracking beam S, which is also related to the linear displacement of the bigrating, x: $\phi \approx S/2D \approx x/R$.

The torsional equation of motion of the mounted bigrating subjected to a time-dependent force $F_x(t)$ may

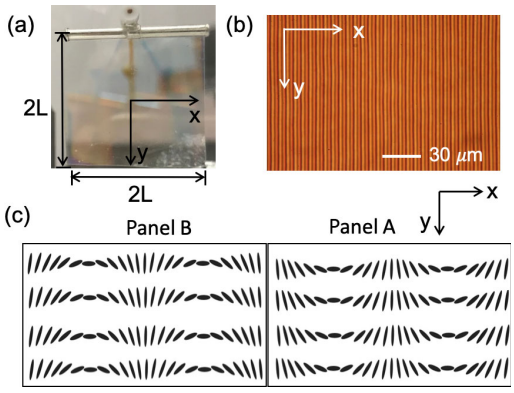

FIG. 2. (a) Diffractive beam rider mounted on the pendulum under unpolarized white light. (b) A panel of the diffractive beam rider under a polarization microscope. (c) Director orientation in the cycloidal diffractive wave plates of opposite sign.

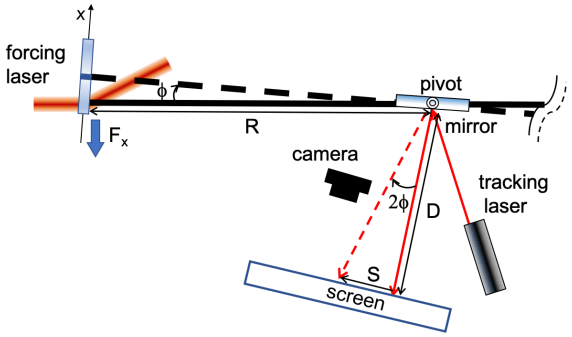

FIG. 3. Partial top view of torsional pendulum with arm of length R that pivots from equilibrium owing to radiation pressure on a bigrating from a forcing laser. Angular displacement ϕ is obtained from the recorded position on a screen of a tracking laser reflected from a mirror at the pivot.

for convenience be expressed as a function of the displacement x rather than the angle:

$$Jd^2x/dt^2 + 2(J/\tau)dx/dt + k_f x(t) = F_x(t)R^2, \quad (4)$$

where $J = (1.16 \pm 0.01) \times 10^{-5}$ kg m^2 is the calculated moment of inertia [32], $k_f = (2\pi/T_0)^2 J = (1.99 \pm 0.04) \times 10^{-8}$ N m/rad is the torsional stiffness of the tungsten filament, $T_0 = 151.8 \pm 0.8$ s is the measured natural oscillation period when $F_x(t) = 0$, and $\tau = (568 \pm 5.5)T_0$ is the measured natural decay time.

To verify the existence of a light-induced restoring force, we measured the step function response of the torsion oscillator, bringing the beam power from zero at $t < 0$ to a value of $P_i = 1.2$ W ($F_0 = 0.39 \pm 0.03$ nN) at $t > 0$, so that $F_x(t) = F_x(x)u(t)$, where $F_x(x)$ may be approximated by Eq. (2) and $u(t)$ is a step function. The instant $t = 0$ corresponds to the state where the excited oscillator passes through equilibrium, $x(t = 0) = 0$. In the linear regime where $|x/w_0| \ll 1$, radiation pressure may be understood as an additional source of torsional stiffness: $k_{\mathrm{RP}} = K_{\mathrm{RP}}R^2 = (2.3 \pm 0.2) \times 10^{-9}$ N m/rad. Thus we expect a corresponding frequency shift, $\Delta\omega = \omega' - \omega_0$, where $\omega_0 = \sqrt{k_f/J} = 2\pi/T_0 = (4.14 \pm 0.02) \times 10^{-2}$ was determined from a measurement of the free oscillation period T_0, and $\omega' = \sqrt{k'/J} = 2\pi/T'$, where $k' = k_f + k_{\mathrm{RP}}$. We measured the period $T' = 141.8 \pm 0.6$ s. A comparison of these stiffness-based $(\omega'|_{k'}) = (4.37 \pm 0.34) \times 10^{-2}$ rad/s and period-based $(\omega'|_{T'}) = (4.43 \pm 0.02) \times 10^{-2}$ rad/s expressions of frequency are in good agreement.

As further evidence of a light-induced restoring force, we compare the amplitude of oscillation before and after the optical step function described above. Instantaneous stiffening may be described as an energy conserving process [28]: $E_0 = (1/2)k_f\phi_{0,\max}^2 = E' = (1/2)k'\phi'^2_{\max}$, where $\phi_{0,\max}$ and $\phi'_{\max} = \phi_{0,\max} - \Delta\phi$ are the respective oscillation amplitudes for $t < 0$ and $t > 0$. Assuming that $\Delta\phi = \Delta x/R \ll 1$, we predict a decrease of the oscillation amplitudes:

$$\Delta\phi = \phi_{0,\max}k_{\mathrm{RP}}/2(k_f + k_{\mathrm{RP}}), \quad (5a)$$

$$\Delta x = x_0 K_{\mathrm{RP}}/2(K_f + K_{\mathrm{RP}}), \quad (5b)$$

where $x_0 = R\phi_{0,\max}$ is the oscillation amplitude for $t < 0$. Inserting foregoing stiffness values and the measured value $x_0 = 1.35$ mm, we predict a value $\Delta x = 0.070 \pm 0.001$ mm (or 5.2% of x_0), which agrees with the measured value of $\Delta x_{\mathrm{meas}} = 0.070 \pm 0.005$ mm.

As a final demonstration of the restoring force model of the bigrating, we experimentally measured parametrically driven damping (or "cooling") by synchronizing laser illumination with the phase of the torsion oscillator. A square wave modulation of the laser power at twice the oscillator frequency was applied (see the inset of Fig. 4) at a beam power $P_i = 1.5$ W and beam size $w_0 = 3.1 \pm 0.05$ mm (i.e., $F_0 = 0.49 \pm 0.04$ nN). The light-induced torsional stiffness corresponds to $k_{\mathrm{RP}} = (1.9 \pm 0.2) \times 10^{-9}$ Nm/rad. The forcing laser was controlled to illuminate the beam rider when the condition $x(t)v(t) > 0$ was satisfied:

$$\tilde{F}_x(t) = \begin{cases} \tilde{F}_x & \text{if } x(t)v(t) > 0, \\ 0 & \text{if } x(t)v(t) \le 0, \end{cases} \quad (6)$$

where $v = \partial x/\partial t$. The modeled response (the dotted line in Fig. 4) making use of Eq. (2) and the fourth order Runge-Kutta numerical technique agrees with the measured displacement (the solid line in Fig. 4), further validating our understanding of the system. The oscillation envelope of the parametrically driven bigrating was found to exhibit exponential decay (the dashed line in Fig. 4):

$$x_{\mathrm{env}}(t) = x_0 \exp(-t/\tau'') \quad (7)$$

with a measured decay time $\tau'' = 1791 \pm 24$ s.

Again using energy arguments and a Hooke's law approximation, we predict the decay time for an arbitrary value of the scaling force, F_0 (or k_{RP}). Using the phased forcing protocol described by Eq. (6) and depicted in the inset of Fig. 4, we note the following sequence for one complete cycle, starting from an oscillation maximum ϕ_a: (a–b) free oscillation for an interval $T_0/4$ with energy $E_{a,b} = (1/2)k_f\phi_a^2$; ($b$–$c$) stiffened oscillation for an interval $T'/4$, reaching an amplitude ϕ_c at point c and an energy $E_{b,c} = (1/2)(k_f + k_{\mathrm{RP}})\phi_c^2 = E_{a,b}$; ($c$–$d$) free oscillation for an interval $T_0/4$ with energy $E_{c,d} = (1/2)k_f\phi_c^2$; ($d$–$e$) stiffened oscillation for an interval $T'/4$, reaching an amplitude ϕ_e at point e with energy $E_{d,e} = (1/2)(k_f + k_{\mathrm{RP}})\phi_e^2 = E_{c,d}$. The period of the full cycle is given by $T'' = (T_0 + T')/2 = 148.4$ s. The algebraic

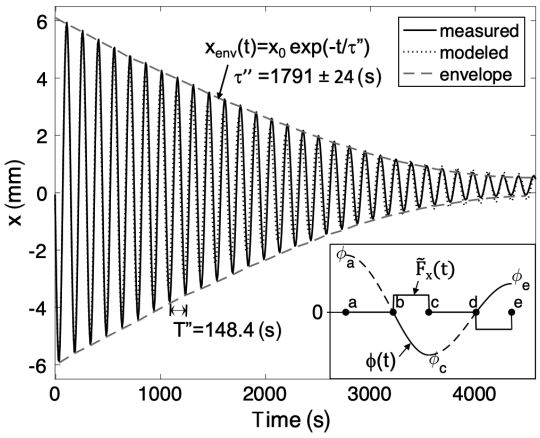

FIG. 4. Parametric cooling of a bigrating using square wave laser modulation at twice the oscillation period. Measured (solid line) and numerically modeled (dotted line) oscillations agree. The oscillation envelope (dashed line) shows exponential decay, with decay time τ''. (Inset) Radiation pressure force $\tilde{F}_x(t)$ synchronized to the oscillation angle $\phi(t)$.

relation between ϕ_a and ϕ_e is readily found: $\phi_e = k_f \phi_a / (k_f + k_{\mathrm{RP}})$. Setting $\phi_e = \phi_a \exp(-T''/\tau'')$, we obtain the decay time,

$$\tau'' = T''/\ln[k_f/(k_f + k_{\mathrm{RP}})], \tag{8}$$

which agrees well with our numerical model and the experimental datum, as shown in Fig. 5.

In summary we reported on experimental demonstrations of self-stabilizing attributes of a diffractive bigrating beam rider. A radiation-pressure-induced restoring force was predicted and experimentally observed by use of a vacuum torsion oscillator. Radiation pressure in effect stiffened the oscillator, resulting in a higher frequency and a smaller amplitude of oscillation. What is more, we demonstrated parametric cooling by synchronizing the radiation pressure with the oscillator state. These results suggest an important technological step forward in the development of laser-driven sailcraft for in-space propulsion. Our one-dimensional bigrating may be generalized in future work

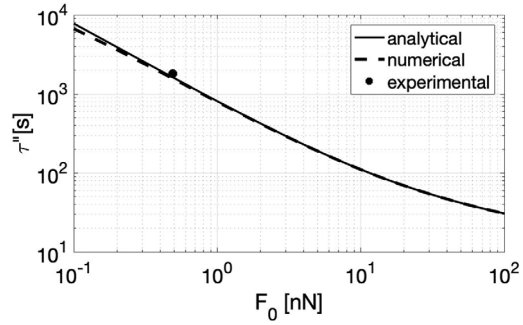

FIG. 5. Parametric cooling decay time τ'' as a function of the transverse radiation pressure force F_0.

to a radial grating or other space-variant designs to achieve three-dimensional optomechananical stability. In general, self-stability may be achieved with either a reflective or a transmissive grating structure, provided it diffracts light toward the center axis. Greater stability occurs for large diffraction angles, but at the expense of less longitudinal force along the axis of the incident beam. Owing to difficulties imposed by the small value of radiation pressure compared to the gravitational acceleration of Earth, we propose demonstration missions either aboard the International Space Station or using CubeSat technology.

We thank the RIT Semiconductor and Microsystems Fabrication Laboratory (SMFL) for providing lab space on the low vibration floor. This research was supported by NASA Innovative Advanced Concepts Program (NIAC) (Grants No. 80NSSC18K0867 and No. 80NSSC19K0975) and the Taiwanese Ministry of Education Study Abroad Scholarship (Grant No. 1061110054). We thank Prateek Srivastava (RIT) for the discussions about bigratings.

*Corresponding author.
grover.swartzlander@gmail.com
†Also at 54 Lomb Memorial Drive, Rochester, New York 14623, USA.

[1] G. Marx, Interstellar vehicle propelled by terrestrial laser beam, Nature (London) **211**, 22 (1966).
[2] R. L. Forward, Roundtrip interstellar travel using laser-pushed lightsails, J. Spacecr. Rockets **21**, 187 (1984).
[3] K. A. Beals, M. Beaulieu, F. J. Dembia, J. Kerstiens, D. L. Kramer, J. R. West, and J. A. Zito, Project longshot: An unmanned probe to Alpha Centauri, U.S. Naval Academy, 1988, https://ntrs.nasa.gov/archive/nasa/casi.ntrs.nasa.gov/19890007533.pdf.
[4] L. Friedman and M. Gould, *Starsailing: Solar Sails and Interstellar Space Travel* (Wiley, New York, 1988).
[5] R. H. Frisbee, Limits of interstellar flight technology, Front. Propul. Sci. **227**, 31 (2009).
[6] P. Gilster, *Centauri Dreams: Imagining and Planning Interstellar Exploration* (Springer Science +Business Media, New York, 2004).
[7] C. R. McInnes, *Solar Sailing: Technology, Dynamics and Mission Applications* (Springer Science +Business Media, New York, 2013).
[8] G. Vulpetti, L. Johnson, and G. L. Matloff, *Solar Sails: A Novel Approach to Interplanetary Travel* (Springer, New York, 2014).
[9] L. Johnson, M. Whorton, A. Heaton, R. Pinson, G. Laue, and C. Adams, NanoSail-D: A solar sail demonstration mission, Acta Astronaut. **68**, 571 (2011).
[10] P. L. Lubin, A roadmap to interstellar flight, J. Br. Interplanet. Soc. **69**, 40 (2016).
[11] P. Daukantas, Breakthrough starshot, Opt. Photonics News **28**, 26 (2017).
[12] G. A. Swartzlander, Jr., Radiation pressure on a diffractive sailcraft, J. Opt. Soc. Am. B **34**, C25 (2017).

[13] Y.-J. L. Chu, E. M. Jansson, and G. A. Swartzlander, Jr., Measurements of Radiation Pressure Owing to the Grating Momentum, Phys. Rev. Lett. **121**, 063903 (2018).
[14] G. A. Swartzlander, Jr., Flying on a rainbow: A solar-driven diffractive sailcraft, J. Br. Interplanet. Soc. **71**, 130 (2018).
[15] P. R. Srivastava, Y.-J. L. Chu, and G. A. Swartzlander, Stable diffractive beam rider, Opt. Lett. **44**, 3082 (2019).
[16] O. Ilic and H. A. Atwater, Self-stabilizing photonic levitation and propulsion of nanostructured macroscopic objects, Nat. Photonics **13**, 289 (2019).
[17] Y. Tsuda and Ikaros Demonstration Team, How *Ikaros* shape is designed: Attitude stability of spinning solar sail, in *Advances in Solar Sailing*, edited by Malcolm Macdonald (Springer, New York, 2014), pp. 45–56.
[18] A. A. Karwas, An unconditionally stable method for numerically solving solar sail spacecraft equations of motion, Ph.D. thesis, University of Kansas, 2015.
[19] E. Popova, M. Efendiev, and I. Gabitov, On the stability of a space vehicle riding on an intense laser beam, Math. Models Methods Appl. Sci. **40**, 1346 (2017).
[20] Z. Manchester and A. Loeb, Stability of a light sail riding on a laser beam, Astrophys. J. Lett. **837**, L20 (2017).
[21] P.-F. Cohadon, A. Heidmann, and M. Pinard, Cooling of a Mirror by Radiation Pressure, Phys. Rev. Lett. **83**, 3174 (1999).
[22] M. Bhattacharya and P. Meystre, Trapping and Cooling a Mirror to Its Quantum Mechanical Ground State, Phys. Rev. Lett. **99**, 073601 (2007).
[23] J. Gieseler, B. Deutsch, R. Quidant, and L. Novotny, Subkelvin Parametric Feedback Cooling of a Laser-Trapped Nanoparticle, Phys. Rev. Lett. **109**, 103603 (2012).
[24] J. Vovrosh, M. Rashid, D. Hempston, J. Bateman, M. Paternostro, and H. Ulbricht, Parametric feedback cooling of levitated optomechanics in a parabolic mirror trap, J. Opt. Soc. Am. B **34**, 1421 (2017).
[25] E. I. Butikov, Pendulum with a square-wave modulated length, Int. J. Nonlinear Mech. **55**, 25 (2013).
[26] D. J. Braun, Optimal Parametric Feedback Excitation of Nonlinear Oscillators, Phys. Rev. Lett. **116**, 044102 (2016).
[27] L. G. Villanueva, R. B. Karabalin, M. H. Matheny, E. Kenig, M. C. Cross, and M. L. Roukes, A nanoscale parametric feedback oscillator, Nano Lett. **11**, 5054 (2011).
[28] E. Butikov, A physically meaningful new approach to parametric excitation and attenuation of oscillations in nonlinear systems, Nonlinear Dyn. **88**, 2609 (2017).
[29] B. Rodenburg, L. P. Neukirch, A. N. Vamivakas, and M. Bhattacharya, Quantum model of cooling and force sensing with an optically trapped nanoparticle, Optica **3**, 318 (2016).
[30] I. Ryger, A. B. Artusio-Glimpse, P. Williams, N. Tomlin, M. Stephens, K. Rogers, M. Spidell, and J. Lehman, Micromachined force scale for optical power measurement by radiation pressure sensing, IEEE Sens. J. **18**, 7941 (2018).
[31] S. R. Nersisyan, N. V. Tabiryan, D. M. Steeves, and B. R. Kimball, The promise of diffractive waveplates, Opt. Photonics News **21**, 40 (2010).
[32] The moment of inertia of the pendulum is determined by $J = M_b(2R)^2/12 + M_c(w^2 + \mathrm{d}^2)/12 + M_r R^2 + M_1 R_1^2 + M_2 R_2^2 = (1.16 \pm 0.01) \times 10^{-5}$ kg m^2, where the torsion bar of mass $M_b = 0.38$ g; center pivot of mass $M_c = 1.05$ g, width $w_c = 5$ mm, and thickness $d = 1$ mm; beam rider with mounting tabs of mass $M_r = 0.45$ g; and two balancing masses on the balancing torsion arm (not shown in Fig. 3) of mass $M_1 = 0.37$ g at distance $R_2 = 0.01$ m away from the pivot and mass $M_2 = 0.48$ g at distance $R_2 = 0.098$ m away from the pivot, respectively. The total mass of the hanging components on the pendulum is 2.73 g.